3

Soft Manipulator Actuation Module – with Reinforced Chambers

Jan Fras[1], Mateusz Macias[1], Jan Czarnowski[1], Margherita Brancadoro[2], Arianna Menciassi[2] and Jakub Głowka[1]

[1]Industrial Research Institute for Automation and Measurements PIAP, Warsaw, Poland
[2]The BioRobotics Institute, Scuola Superiore Sant'Anna, Pontedera (PI), Italy

Abstract

During the integration and data-fusion algorithms tests it turned out that the initial manipulator prototype, described in Chapter 2, had a number of drawbacks emerging from its structure and resulting in high actuation non-linearity and low sensing capabilities. In this chapter we show how the internal distortions in the initial design influence the manipulator behaviour and the sensory readings, and then we propose new designs that solve those issues. A braided actuation chamber instead of the overall module braiding concept is presented together with the manufacturing technology and experimental characterization of the actuation module. The idea of using multiple actuation chambers and the division of the central stiffening chamber into distributed stiffening chambers is also presented.

3.1 Introduction

The braided sleeve used for the initial design of the STIFF-FLOP manipulator rendered itself to be a good solution (Chapter 2). The actuation chamber's radial expansion were not being observed and the modules were still able to bend, elongate, and squeeze. The problem seemed to be solved; however, the

sensors integration process has shown that the external inflation of the chambers during actuation is a bit more complex and the braided reinforcement limits only the symptoms of the problem. Moreover, since such a solution limits the external expansion, it intensifies the deformation of the actuation chambers in an inward direction. In addition, the interaction between the silicone body of the manipulator and the external reinforcement structure introduces some new undesired and unexpected effects. Effects that have been noticed are: non-linear actuation, distortion of the internal sensors readings (mainly the curvature and length sensors as they are based on the structural deformation of the manipulators' body), complex control, and modeling.

In the following sections we analyze those effects and their relation to the initial braiding solution. The analysis is derived from several observations of the manipulators' behaviour during actuation tests. For that a dedicated module has been used. One of its ends was cut and sealed with a transparent tile that allowed for the observation of its interior.

3.1.1 Change of the Chamber Cross Section Area

As the actuation chamber is simply an empty cylindrical channel in the silicone material, application of pressure into it causes it to expand radially. That effect influences the cross section area of the activated actuation chamber and the area of the other chambers' cross sections as well. As the force resulting from pressure acting inside the chamber, depends not only on the pressure but also on the cross section of the chamber the mentioned increase of the chamber dimensions causes the force to change its value in a non-linear way as a function of pressure.

3.1.2 Chamber Cross Section Center Displacement

In the initial design the cross section of the actuation chamber was semi-circular. Its shape is not retained during the actuation due to the material deformation constrained by the braiding and the overall module cross section geometry. That causes the chamber cross section geometry and its location to change when the pressure changes. Consequently the position of the actuation cross section moves in relation to the manipulator central axis depending on the pressure inside the chamber. Actuation of two chambers simultaneously results in a lower bending angle than the single-chamber actuation with the same pressure. The cause of this situation is presented in Figure 3.1. The explanation is that the bending deformation of the manipulator results from

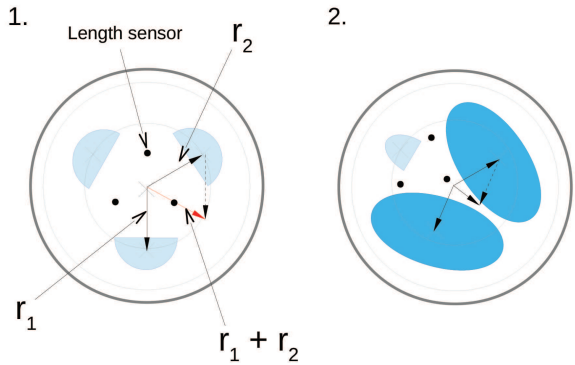

Figure 3.1 Deformation of the module cross section during actuation. The two-chamber actuation case results in their expansion and their axis displacement that results in lowering the pressure-dependent bending moment in the cross section.

bending moment generated by actuation chambers. This in turn is caused by the forces resulting from internal actuation pressures. As the pressure value p is constant at every point of the chamber volume, the value of the internal force acting on a certain chamber cross section center can be easily calculated as $F_i = A_i p$, where A_i is the area of the cross section [1]. Denoting vectors from the center of the cross section to centers of each chamber as $\overrightarrow{r_1}$ and $\overrightarrow{r_2}$, the resulting bending moment M in the considered cross section, the module can be expressed as Equation (3.1).

$$M_i = (\overrightarrow{r_1} + \overrightarrow{r_2})F_i \tag{3.1}$$

In Figure 3.1, the situation with two simultaneously actuated chambers is presented. The shape of the chamber cross section is deformed and its geometrical center moves. Due to the passive module geometry, the chamber cross section shifts towards the module center and as a result the length of the net vector $\overrightarrow{r} = \overrightarrow{r_1} + \overrightarrow{r_2}$ is decreased. That in turn leads to a reduction in the value of the net bending moment deforming the module Equation (3.1).

3.1.3 Friction between the Silicone Body and Braided Sleeve

As mentioned in the chapter introduction, the braided sleeve, beside constraining the ballooning effect, also influences other manipulator properties. The final shape of the manipulator depends on the previously applied pressures and in particular on the chamber actuation order. The friction force caused by the first chamber actuation limits the second chamber expansion

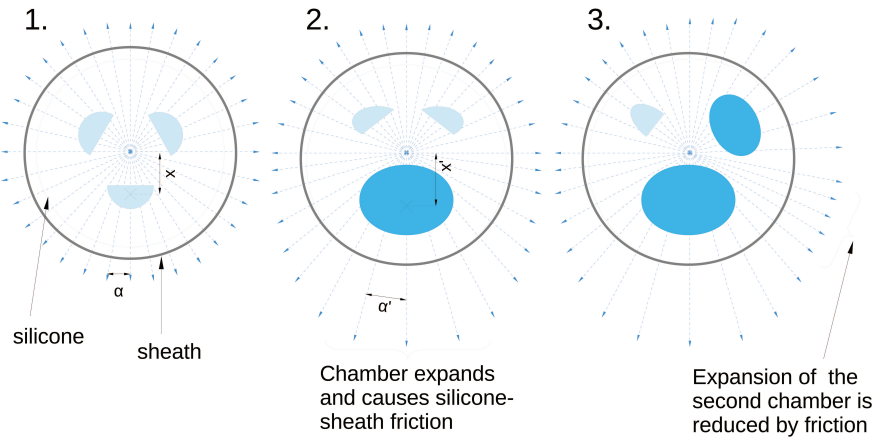

Figure 3.2 Module cross section during a two-module actuation sequence. (1) presents the cross section with no pressures applied to the chambers. No friction between the sheath and silicone occurs. In (2), pressure is applied to one of the chambers. The chamber expansion causes the external sheath to make contact with the module body. The second chamber is constrained by the inflation and friction with the sheath (3).

and reduces its elongation and thus its impact on the manipulator. This effect is clearly observed in case of two chambers subsequent actuation Figure 3.2. Applying the pressure to a chamber makes it expand and increase its cross section. Due to that, the module surface is pressed to the reinforcement from the inside. When the second chamber is actuated, its expansion is significantly smaller than the first one since the space for the expansion is already occupied by the initially pressurized chamber that was expanding without such constraints. Pushing it away requires moving the silicone pressed to the braiding, which requires additional force due to the friction. Consequently the second chamber grows less than the first one and due to this, the pressure-related elongation is also smaller. As an effect, the module is not capable of efficient bending in the directions requiring multiple chambers to be actuated, which greatly impacts the shape of an achievable workspace when using constant pressure.

3.1.4 Sensor Interaction

One of the sensors developed in the STIFF-FLOP project used for manipulator configuration detection is a curvature sensor composed of three parallel-length sensors [2], that are made of a light fiber slighting in a dedicated

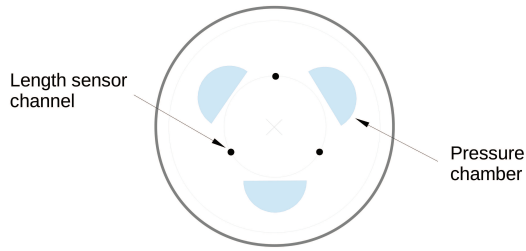

Figure 3.3 The length sensor channel placement presented in a module cross section. The channels are placed on a circle coaxial with the module axis of symmetry.

hollow. Each individual fiber is attached at the modules' tip so that any elongation of the module causes the fibers to be pulled inside its body. That in turn makes the end of the fiber change its distance form a light intensity detector and finally allows the lenght of the particular part of the module to be calculated. The sensors are embedded into the module with axial symmetry Figure 3.3. and are assumed to be parallel to the module central axis. Any deviation from that is a source of error. The internal inflation of the chambers disrupts this assumption, as the readings from the sensors are highly dependent on the pressure and not only on the shape of the manipulator. The curvature of the module is assessed using the individual lengths of the sensors, and so that is a significant issue and makes sensor fusion a complex task.

Another issue is that the braiding structure surrounding the manipulators' body is undesired due to its roughness, which may cause harmful interaction with the patients' tissue and an array of tactile sensors that was considered to be integrated with the manipulator's surface. Integration of such sensors rendered itself to be much easier done in case of the homogenous silicone body itself than in the braided reinforcement. More information on this type of sensors can be found in [3].

3.2 Proposed Improvements

To reduce the issues described in the introduction, radial expansion of each individual chamber has to be constrained. Any changes to the cross section geometry are undesired too, as they may result in a less linear actuation process. The idea we propose is to make the chamber geometry more stable by employing braiding around each chamber instead of constraining the external expansion of all chambers with one external sheath.

3.2.1 Possible Solutions

The external braided sleeve embedded to solve the undesired module expansion demonstrated to provide effective radial expansion constrains allowing the longitudinal chambers expansion at the same time, but due to a number of undesired effects another solution has to be proposed. Similar examples of constraint can be found in the work by Whitesides et al. who, facing the same ballooning effect [4], developed a manufacturing process which allows the internal patterning of the chambers (PneuNets), reducing the lateral space available to produce outward expansion [5]. A different and simpler approach has been proposed by Brock et al. Their solution is a squared-section chamber reinforced with inelastic yarns placed all around [6]. Such an approach is simpler and faster to manufacture, and provide a similar performance to the first one.

3.2.2 Design

The first solution used semi-cylindrical chambers. This approach would ensure that the chamber circumference is constant during the actuation, and so limit the radial expansion. In general, the cross section geometry would, however, still not be constant as the chamber behaviour during actuation will aim to maximize its cross section area, and will finally reach a circular cross section shape. This effect has been discussed in more detail in [7]. Therefore in the proposed solution, the semicylindrical chambers have been substituted with cylindrical ones [8]. Such a change would also simplify the manufacturing process. The concept is presented in Figure 3.4.

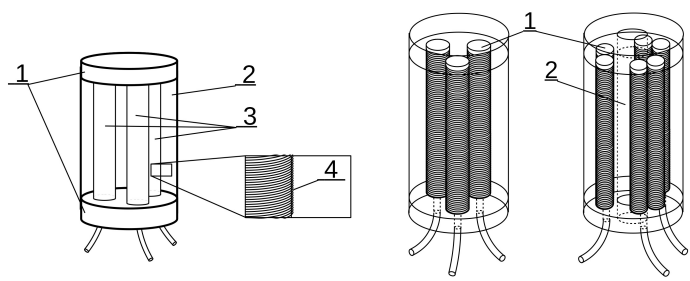

Figure 3.4 Improved design concept. (a) the module overview, 1 - top and bottom of the module made of stiff silicone, 2 - module body made of soft silicone, 3 - actuation chambers, 4 - helical thread reinforcement, (b) 1 - actuation chambers, 2 - empty central channel.

The final version of the manipulator was built using pairs of chambers working together and an empty channel for passing the pressure pipes to modules stacked one on top of another Figure 3.4(b). The requirement of empty space inside the module forced the chambers to have a smaller actuation volume and experiments have shown that such a change requires higher pressures and significantly reduced final motion capabilities of the manipulator. In order to preserve the desired actuation area, the singular actuation chambers were substituted with multiple chambers connected inside the module [9]. For the same reason the stiffening chamber has been split to three smaller channels located between the actuation chambers. Such an operation allowed to create the central channels, but also improved the stiffening performance as its area moment of inertia increased. An assembled module is presented in Figure 3.5(c) and a modified module with a central hollow channel, doubled actuation chambers, and three individual stiffening chambers is presented in Figure 3.6.

(a) (b) (c)

Figure 3.5 Initial manufacturing approach. (a) chambers manufacturing - winding a thread on prefabricated silicone cylinder, (b) body moulding, (c) imperfections caused by the stresses introduced during winding process.

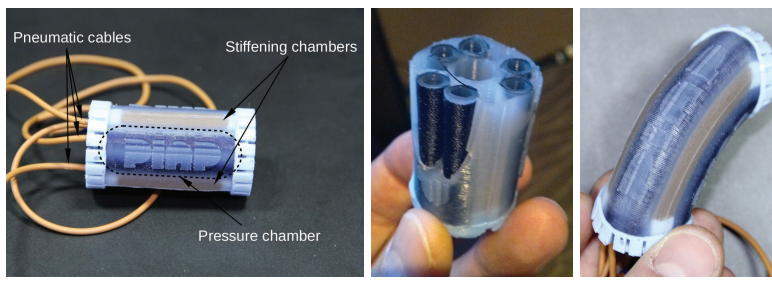

(a) (b) (c)

Figure 3.6 The STIFF-FLOP module. (a) overview, (b) actuation chambers disclosed, reinforcing thread visible, (c) actuated module.

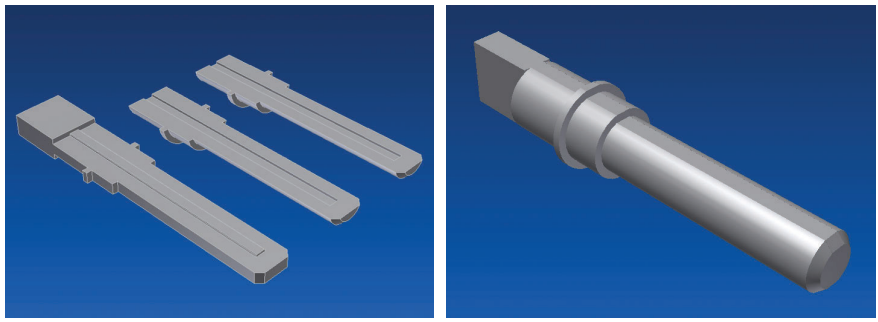

(a) (b)

Figure 3.7 Mold core. (a) parts of the core, (b) core assembly.

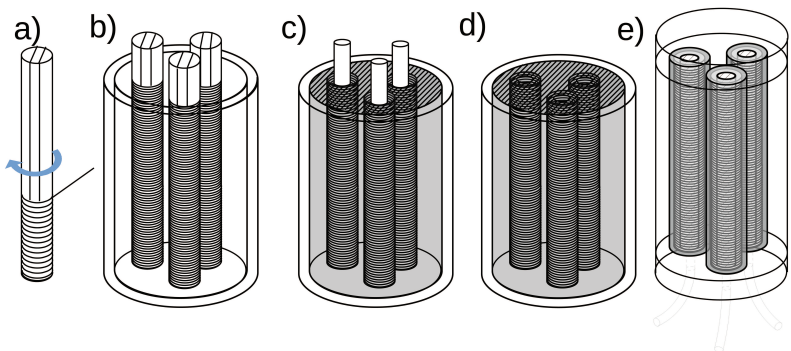

Figure 3.8 Module manufacturing steps. (a) Thread application on a rod, (b) body part molding, (c) replacement of the initial rod with a smaller-diameter one, (d) internal chamber layer created, (e) sealing of the manipulators' tip and bottom.

3.3 Manufacturing

The improved manipulator is manufactured in several molding steps. For that purpose, a set of 3D printed moulds is used. The process has been evolving during the project but the idea behind it remained the same. The main issue is to create sealed cylindrical chambers with the reinforcement incorporated into their walls and to embed them into the manipulator body. Originally the thread was applied onto prefabricated silicone cylinders (Figure 3.5(a)) and such cylinders were then sealed with the silicone material forming the module (Figure 3.5(b)).

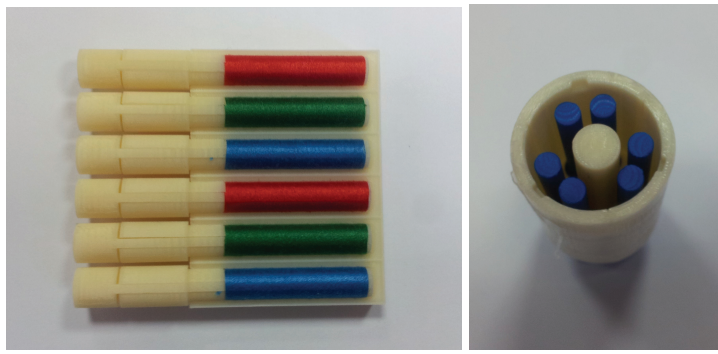

(a) (b)

Figure 3.9 Improved manufacturing approach. (a) molding cores wrapped with reinforcing thread, (b) wrapped cores in the main body mold.

Such a method was very imprecise due to the fact that the soft structure that the thread was applied on and the tension required for the proper thread placement introduced a lot of stresses into the silicone material. As a result the material was pressed in the direction of the thread application and caused many irregularities in the reinforcement structure. This effect can be observed in Figure 3.5(c) as a small difference in the pitch of the reinforcement. The material was pressed out between the reinforcement cycles. Another issue is that the friction of the chamber pressed by the applied thread made it impossible to remove the core from inside without damaging the chamber structure and forced us to solve that issue by designing a three-part core that is removed part by part Figure 3.7. The central part is removed as the first one, while the other parts protect the silicone layer. After the internal part is removed, the remaining parts can be removed without any resistance.

Due to the above issues, the technology has been improved. The manufacturing steps have been reordered as presented in Figure 3.8. The initial step is to create the reinforcement on a rigid rod (Figure 3.9). Since the rod is rigid, the thread does not introduce any significant stress into the structure of the chamber. Moreover, the wrapping process is very simple and can be easily automated, as every cycle of the reinforcement stacks onto the previous one. To simplify the core removal that is done in the next steps, the core construction has ben inherited from the previous manufacturing approach and consists of three parts. When the core is wrapped, it is inserted into the main mold and the manipulator's body is created. Once the silicone is cured, the cores are removed—part by part, the internal part at first, and

then the sides, so that the thread remains attached to the body. After that, the hollow chambers with the thread attached to their walls are filled with uncured silicone and a set of smaller cores is inserted inside the mold. This is for creating a layer of silicone that corresponds with the prefabricated silicone cylinders from the initial approach. After curing, the structure of the main part of the module is ready. For the last step the top and the bottom of the module is closed with a stiff silicone.

3.4 Tests

The new version of the module has been tested in order to compare its performance with the previous design. The assumed improvements has been observed. In particular the ballooning effect has been successfully limited, while the internal structure deformation was not observed.

3.4.1 Pneumatic Actuation

Pneumatic actuation was the primary actuation method in the STIFF-FLOP project. Thus, both designs have been tested in terms of the bending angle as a function of pressure. Single- and 2-chamber actuation scenarios have been examined. The test setup is presented in Figure 3.10. The plots from Figures 3.11(a) and 3.11(b) present the results for the old and new design, respectively. The test shows that the new design works with a wider range of actuation pressures for a similar range of bending angles. This effect is caused by the efficient limitation of the ballooning effect. In the initial design the chambers were able to extend radially, which resulted in the cross sectional

Figure 3.10 Test configuration for measuring module bending by applying pressure into module chambers.

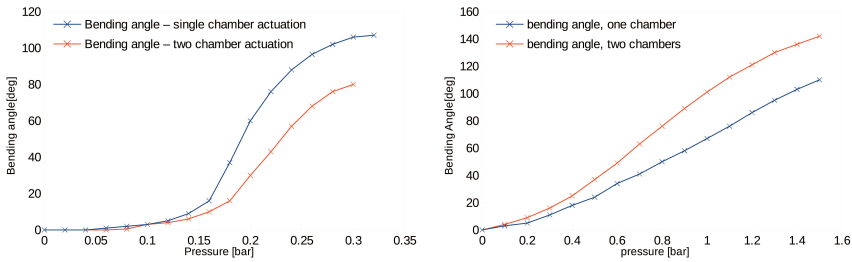

(a) (b)

Figure 3.11 Bending angle achieved for certain values of pressure applied for: (a) the old design, (b) the new design.

actuation chamber area growth. Such a growth was causing the actuation force to be higher for the same pressure value. That resulted in greater sensitivity with increasing pressure, while ideally, with non-expanding chambers, the relation between the achieved bending angle and pressure applied to the chamber should be linear [10]. The observed improvement in terms of linearity confirms the successful limitation of the internal ballooning effect.

Another observed difference is that for the previous design, the resulting bending angle values are lower in case of 2-chamber actuation than in the case with single-chamber actuation. The reason is probably the effect described in Section 3.1.2. The new design does not display such behaviour—for the same pressures applied, the bending-angle values for 2-chamber actuation are higher than one-chamber actuation which meets our expectations.

Figure 3.12 Test configuration for measuring module bending by injection of a certain amount of incompressible liquid.

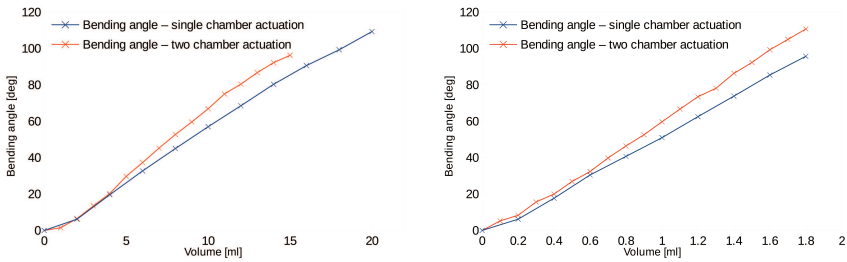

(a) (b)

Figure 3.13 Bending angle achieved for certain values of liquid volume injected into chambers of: (a) the old design, (b) the new design

3.4.2 Hydraulic Actuation

Both designs have also been tested in the hydraulic actuation scenario. The main difference in such case is that it is not the pressure but the volume of the actuation chamber that is controlled. Such a test quantitatively shows the ballooning effect observed in the previous design. The test configuration used for this experiment is presented in Figure 3.12. The bending angle as a function of volume injected into the actuation chamber for the previous and the new design are presented in Figures 3.13(a) and 3.13(b), respectively. It can be observed that drastically lower volumes of liquid are required by the new module to achieve a certain bending-angle. The relative increase of volume to achieve certain bending angle values is approximately ten times greater for the previous module (2500% compared to 250% for the bending angle of 110 degrees).

3.4.3 External Force

In order to assess the reinforcement impact on the passive behaviour of the manipulator, the bending angle and the elongation caused by the application of external force has been measured for two similar modules: with and without braiding around the actuation chambers. The test configurations are presented in Figures 3.14(a) and 3.14(b) and the resulting plots in Figures 3.15(a) and 3.15(b). The experiment shows that there are no significant differences between those two modules, suggesting that the influence of the reinforcement on the manipulator behaviour under external forces can be neglected.

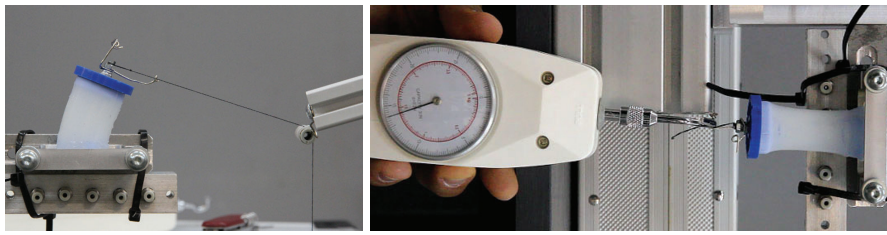

(a) (b)

Figure 3.14 (a,b) Test setup for measuring the individual-chamber braiding influence on module bending elongation by external force, respectively.

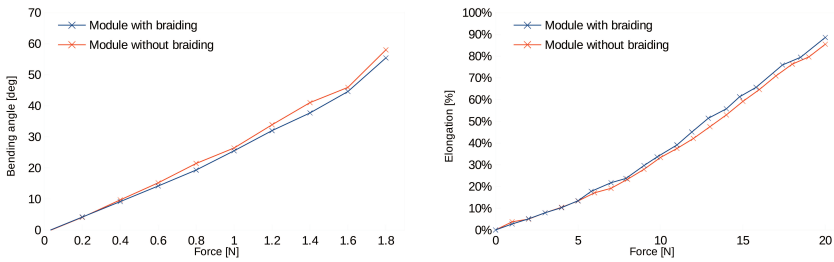

(a) (b)

Figure 3.15 (a,b) Bending angle and elongation respectively, achieved by the modules with and without individual-chamber reinforcement when applying external force.

3.5 Stiffening Mechanism

The design of the final arm has been developed starting from the new approach of manufacturing described in this chapter. This method of module fabrication allows obtaining chambers that can only elongate in response to the pressure, as they have a circular cross section and they are enveloped by an inextensible thread wrapped around their walls. This thread is completely embedded into the matrix of the silicone. Such design has been used to build the modules composing the STIFF-FLOP manipulator; in particular two versions of chamber arrangements (i.e., basic and optimized) have been developed and integrated with the control system. The employed stiffening mechanism is the granular jamming-based mechanism (described previously); in order to leave a free lumen in the module for the passage of the pipes from and to other modules, the granular jamming chambers are distributed around the centre, similar to the actuation chambers.

3.5.1 Basic Module Design

The basic version is composed of three actuation chambers (with integrated thread) and three stiffening chambers, organized in an alternating fashion along the cylindrical STIFF-FLOP module wall parallel to the longitudinal axis of the module. The section view in Figure 3.16 (left) shows the equal distribution of all the chambers around the central axis of the module. The stiffening chambers host the particles for the granular jamming mechanism enclosed in a custom-made latex membrane. Overall, each module has three fluidic pipes (positive air pressures) that feed air into the actuation chambers (inflation/deflation) for the purpose of actuation and another three pipes to allow controlling the vacuum levels in the stiffening chambers. According to this design a three-module manipulator has been built and integrated with force sensors (refer to Part II of this book). This manipulator is composed of two modules with an integrated stiffening mechanism (I. and II.) and one without (III.), as shown in Figure 3.16 (right).

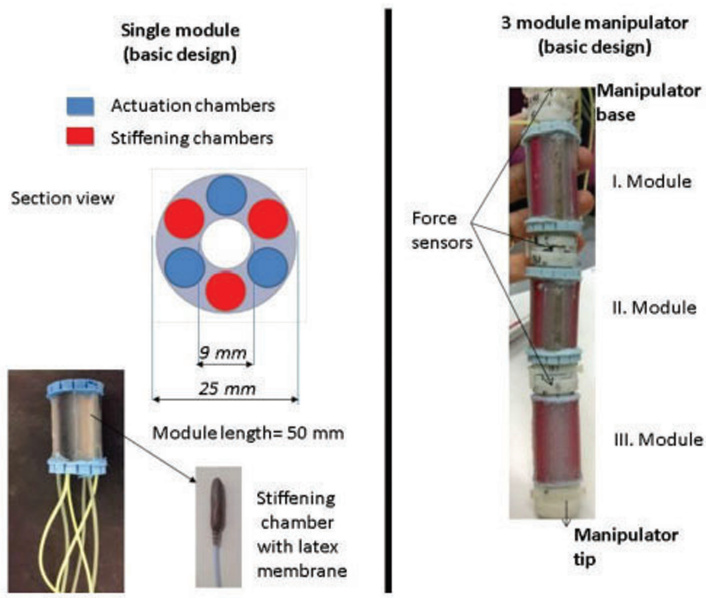

Figure 3.16 The basic module design: Left: section view of the chambers distribution and integration of the granular jamming chamber with latex membrane. Right: assembled 3-module manipulator. The total number of pipes from the manipulator is equal to 15 (6 for I. and II. module and 3 for the III. module).

3.5.2 Optimised Module Design

In order to have more efficient actuation stiffening and a minimal total number of pipes per module, an optimized version of the single module design has been developed. To maximize the effective area of the input pressure, still keeping the same size of the inner lumen and circular chamber cross section, two cylindrical actuation chambers per DoF are used. These two chambers are internally connected: so even if this module has six actuation chambers, the actuation pipes required for the pressurization of the module are still equal to three (since two chambers are always actuated at the same time). The cross section area of the stiffening chambers has been changed from a circular shape into the shape depicted in Figure 3.17 (section view), which allows occupying the maximum volume left in the module for the allocation of the stiffening mechanism. A stiffening chamber experiences a collapse of the lateral surface when a negative pressure (vacuum) is applied to the chamber, therefore a shape like the one in the cross section of Figure 3.17 (left) will assist the effect of the vacuum on the granular media by collapsing

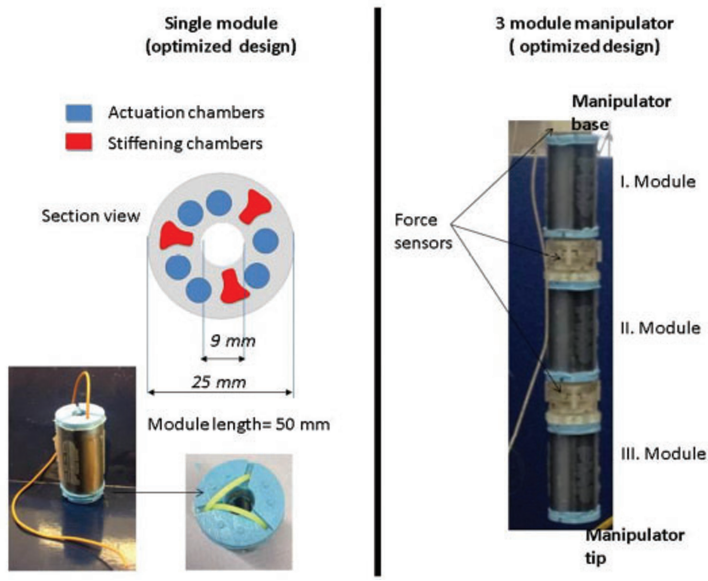

Figure 3.17 The optimised module design: Left: section view of the chambers distribution and single module with integrated granular jamming chambers without membrane and connected together. Right: assembled 3-module manipulator. The total number of pipes from the manipulator is equal to 11 (4 for I. and II. module and 3 for the III. module).

the chamber walls on the granules. In this new optimized design, the granules for jamming are not enclosed in a latex membrane anymore, but are directly in contact with the chamber's wall in the silicone matrix. Furthermore, the three stiffening chambers have been connected all together (see Figure 3.17 (left) module section view) because the vacuum is always applied simultaneously to all the stiffening chambers. The result is a module which has three actuation pipes for motion/bending and just one pipe for controlling the stiffness. With such design, a 3-module manipulator has been integrated with force sensors and interfaced with the control system for tests.

3.6 Conclusions

The new design proved its ability to successfully limit all the issues observed in previous module designs. This goal has been achieved by redesigning the actuation chamber and moving the reinforcement from outside the module to around each individual chamber. This allows for easier data fusion and modeling, and influences positively other areas of the STIFF-FLOP projects. Such a solution is not application-specific and similar actuators have been embedded in other soft robotics systems for manipulation, grasping, prosthetics and locomotion [7, 10, 11].

Acknowledgement

The work described in this chapter is supported by the STIFF-FLOP project grant from the European Commission's Seventh Framework Programme under grant agreement 287728. This project is also partly supported from funds for science in the years 2012–2015 allocated to an international project cofinanced by Ministry of Science and Higher Education of Poland.

References

[1] Fraś, J., Czarnowski, J., Maciaś, M., and Główka, J. (2014). *Static Modeling of Multisection Soft Continuum Manipulator for Stiff-flop Project*. Berlin: Springer.

[2] Searle, T. C., Althoefer, K., Seneviratne, L., and Liu, H. (2013). "An optical curvature sensor for flexible manipulators," in *Proceedings of the Robotics and Automation (ICRA)*, Hong Kong, 6–10.

[3] Sareh, S., Jiang, A., Faragasso, A., Noh, Y., Nanayakkara, T., Dasgupta, P., et al. (2014). "Bio-inspired tactile sensor sleeve for surgical soft manipulators," in *Proceedings of the 2014 IEEE International Conference on Robotics and Automation (ICRA)*, Hong Kong, 1454–1459.

[4] Martinez, R. V., Branch, J. L., Fish, C. R., Jin, L., Shepherd, R. F., Nunes, R. M. D., et al. (2013). Robotic tentacles with three-dimensional mobility based on flexible elastomers advanced materials. *WILEY-VCH Verlag* 25, 205–212.

[5] Shepherd, R. F., Ilievski, F., Choi, W., Morin, S. A., Stokes, A. A., Mazzeo, A. D., et al. (2011). Multigait soft robot. *Proc. Natl. Acad. Sci. U.S.A*. 108, 20400–20403.

[6] Deimel, R., and Brock, O. A. (2014). "Novel type of compliant, underactuated robotic hand for dexterous grasping," in *Proceedings of the Robotics: Science and Systems*, Berkeley, CA.

[7] Fras, J., Noh, Y., Wurdemann, H. A., and Althoefer, K. (2017). *Soft Fluidic Rotary Actuator with Improved Actuation Properties*. Rome: IEEE.

[8] Fraś, J., Czarnowski, J., Główka, J., and Maciaś, M. (2017a). *Soft Manipulator*. PL Patent PL226535.

[9] Fraś, J., Czarnowski, J., Główka, J., and Maciaś, M. (2017b). *Soft Manipulator Module*. PL Patent PL225988.

[10] Fraś, J., Czarnowski, J., Maciaś, M., Główka, J., Cianchetti, M., and Menciassi, A. (2015). "New stiff-flop module construction idea for improved actuation and sensing," in *Proceedings of the International Conference on Robotics and Automation* (Rome: IEEE), 2901–2906.

[11] Fraś, J., Maciaś, M., Czubaczyński, F., Sałek, P., and Główka, J. (2016). Soft flexible gripper design, characterization and application," in *Proceedings of the International Conference SCIT, Warsaw, Poland* (Berlin: Springer).